

Supplementary Materials for

Chiral switching in biomineral suprastructures induced by homochiral L-amino acid

Wenge Jiang, Michael S. Pacella, Hojatollah Vali, Jeffrey J. Gray, Marc D. McKee*

*Corresponding author. Email: marc.mckee@mcgill.ca

Published 1 August 2018, *Sci. Adv.* **4**, eaas9819 (2018)

DOI: 10.1126/sciadv.aas9819

The PDF file includes:

Supplementary Text

Fig. S1. Growth of hierarchically organized vaterite suprastructures stabilized by amino acids.

Fig. S2. Chiral switching of hierarchically organized vaterite helicoid suprastructures in the presence of single chiral D-enantiomer of amino acid (D-Asp).

Fig. S3. Size-related uniformity among vaterite helicoids having chiral switching when grown in the presence of a single chiral enantiomer of amino acid (D-Asp) at low supersaturation conditions.

Fig. S4. Growth evolution of hierarchically organized vaterite helicoids with respect to size and height.

Fig. S5. Multilayering within chiral vaterite helicoids.

Fig. S6. Instability of adjacent rotated vertical vaterite platelets caused by the addition of chiral amino acid enantiomer.

Fig. S7. Chiral switching by platelet layer-by-layer rotation correlates with size/growth of very large helicoids.

Fig. S8. Layer-by-layer growth models as a potential general strategy for switching chiral structures as observed in biology.

Fig. S9. Prediction of three as-yet unfound forms of human pathologic vaterite otoconia based on the vaterite helicoid chiral switching growth model.

Legend for movie S1

Reference (53)

Other Supplementary Material for this manuscript includes the following:

(available at advances.sciencemag.org/cgi/content/full/4/8/eaas9819/DC1)

Movie S1 (.mov format). Animation showing chiral switching in vaterite helicoidal suprastructures occurring by a vertical platelet layer-by-layer rotation mechanism in the presence of a single chiral enantiomer of acidic amino acid.

Supplementary Text

The nucleation and growth of vaterite helicoids

The evolution process of vaterite helicoids can be separated into nucleation events (related to the number of helicoids formed), and growth events responsible for helicoid size, both of which are regulated by the extent of supersaturation (σ) of the reaction solution⁵³. Nucleation rate J_n is related to σ^2 as described in Equation 1, but growth speed v is proportional to σ as shown in Equation 2. Thus, vaterite helicoid growth can predominate, with no nascent vaterite helicoid nucleation, from a solution with low supersaturation (where calcium and carbonate ions are equimolar; 1.1 mM). Under these circumstances, nucleated vaterite helicoids all grow simultaneously and have uniform growth rates and size for the whole growth process, with all having the same chirality (fig. S3). However, with higher supersaturation (where calcium and carbonate ions are equimolar; 2.5 mM), nucleation of vaterite totoids is preferred (over growth) in the reaction solution. Thus, besides the growth of existing vaterite helicoids at an early stage induced by L-Asp enantiomer, nascent small vaterite helicoids can additionally nucleate in the system; this provides for a full range of helicoid sizes (with their respective alternating chirality, with transitional achiral helicoids) which leads to the co-existence of different enantiomorphs at any given time (Fig. 3, main text), as occurs in biology (*e.g.* gastropods and coccolith skeletons).

Nucleation rate J_n

$$J_n = A \exp(-B\alpha^3/\sigma^2) \quad (1)$$

Where A is kinetic constants, B is coefficient, and α is the interfacial free energy.

Growth speed v becomes

$$v = \Omega\beta C_e \sigma \quad (2)$$

where Ω is the volume per molecule. The parameter β is the kinetic coefficient, and C_e is the equilibrium reactant concentration. All are constant.

Supplementary Figures

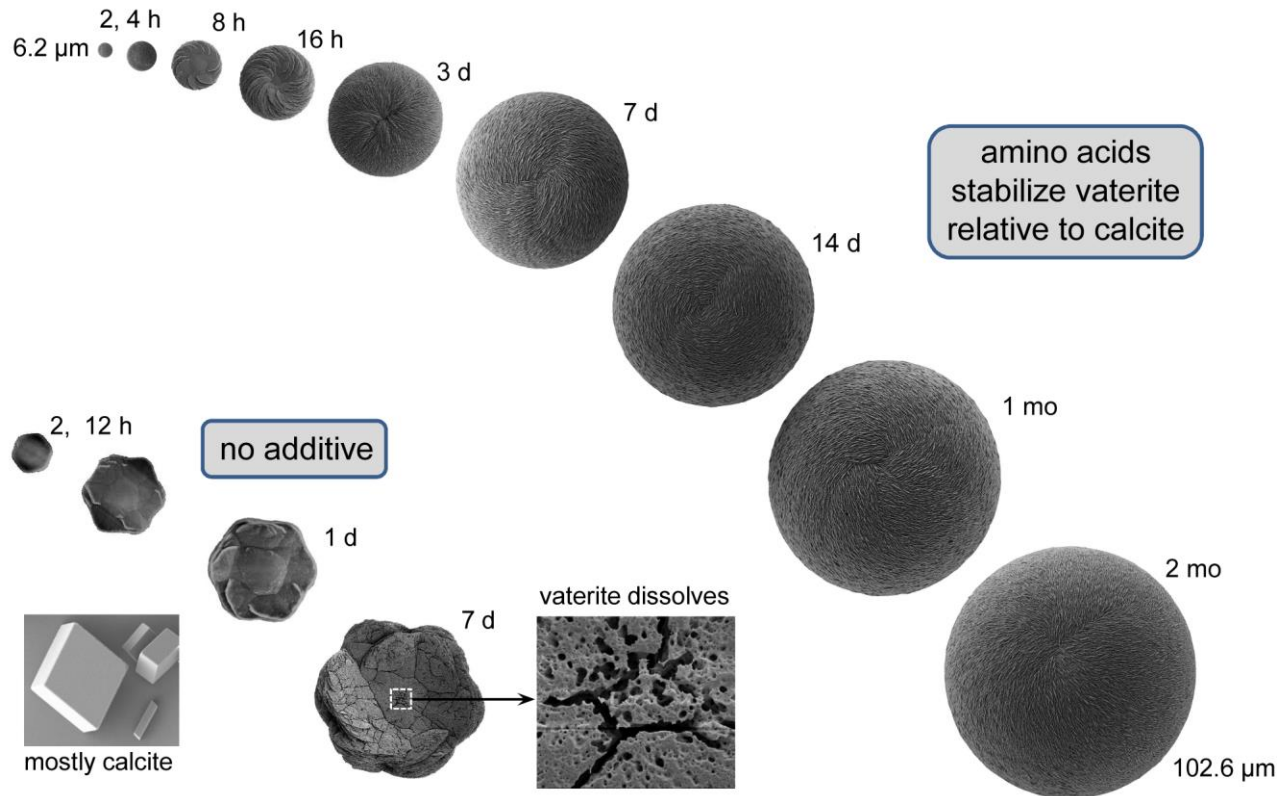


Fig. S1. Growth of hierarchically organized vaterite suprastructures stabilized by amino acids. Scanning electron microscopy (SEM) showing the growth in size and stabilization of vaterite helicoid suprastructures in the presence of 20 mM L-Asp compared with rarely formed and unstable hexagonal vaterite crystals (most are characteristically rhombohedral with symmetric calcite crystal) in the absence of amino acids.

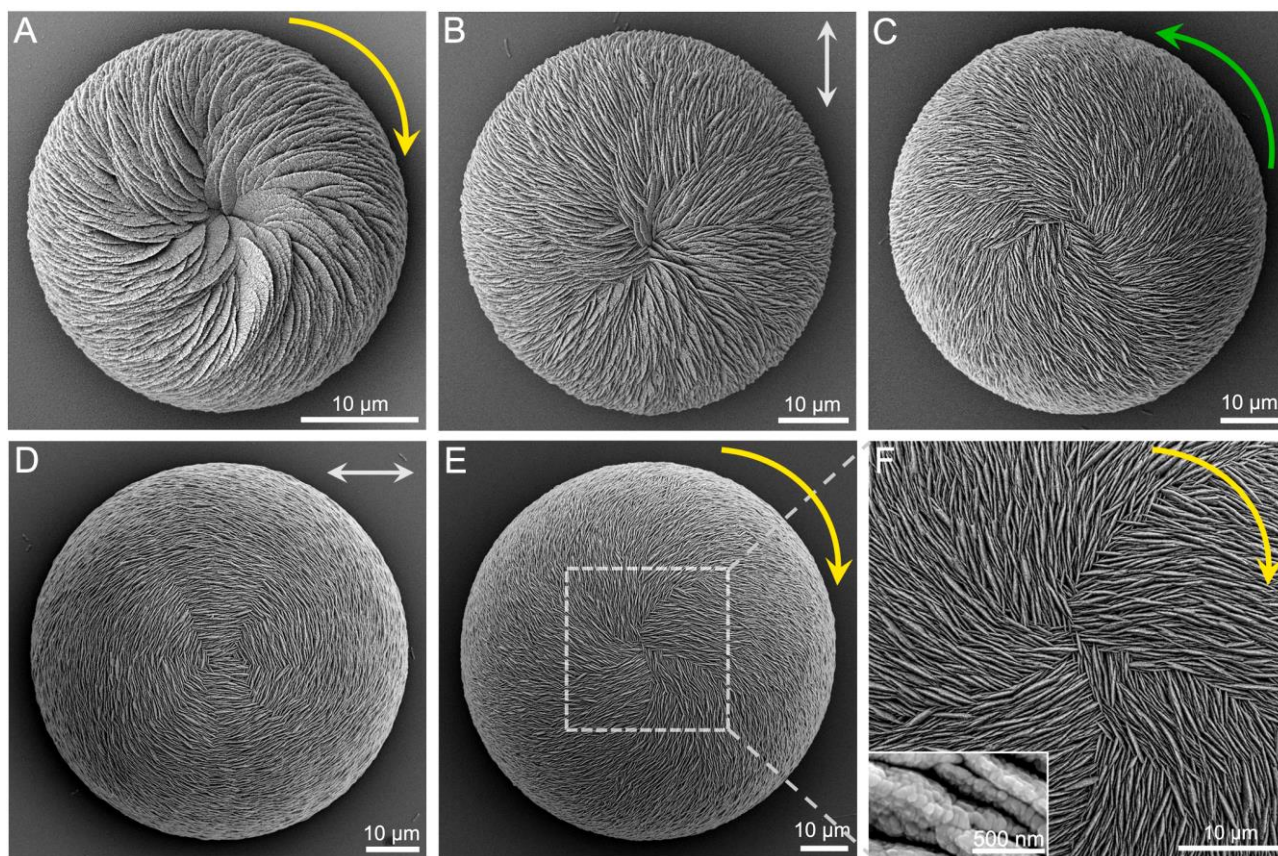


Fig. S2. Chiral switching of hierarchically organized vaterite helicoid suprastructures in the presence of single chiral D-enantiomer of amino acid (D-Asp). (A) SEM images of an initial vaterite helicoid with left-handed (clockwise) spiraling chirality (yellow arrow) in the presence of D-Asp (24 hours of growth). With development, chiral switching appears from an achiral vaterite helicoid with straight-radiating (gray double-headed arrow) vertical vaterite platelets relative to the helicoid centroid at 3 days of growth (B), to the right-handed (counterclockwise, green arrow) spiraling orientation at 1 week of growth (C), to transitional achiral helicoids with horizontal-surrounding vertical platelet orientation (gray double-headed arrow) at 2 weeks (D), and then to the left-handed (clockwise, green arrow) orientation at 1 month (E) with interlacing vertical platelets assembled into a suprastructure (F). Platelets have subunit nanostructure (inset, F).

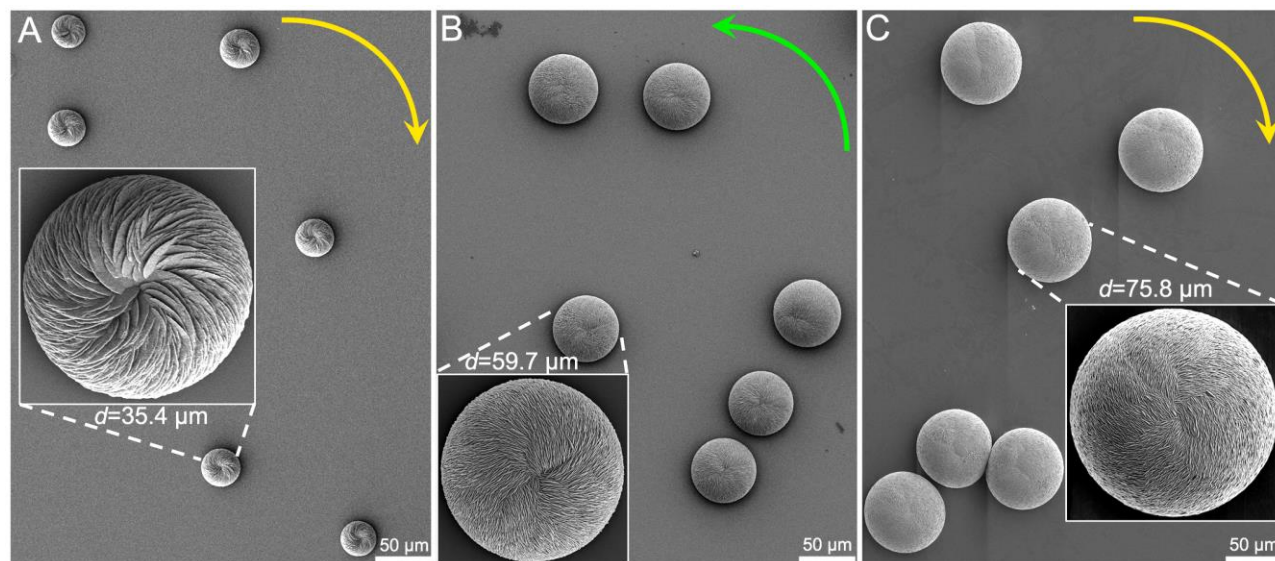


Fig. S3. Size-related uniformity among vaterite helicoids having chiral switching when grown in the presence of a single chiral enantiomer of amino acid (D-Asp) at low supersaturation conditions. Low and high (insets) magnification SEM images of (A) small vaterite helicoids grown for 36 hours, (B) medium vaterite helicoids grown for 2 weeks, and (C) large vaterite helicoids grown for 2 months, with all showing uniform and reproducible either right-handed (counterclockwise, yellow arrow), left-handed (clockwise, green arrow), and right-handed (counterclockwise, green arrow) orientations, respectively, within in one viewing area.

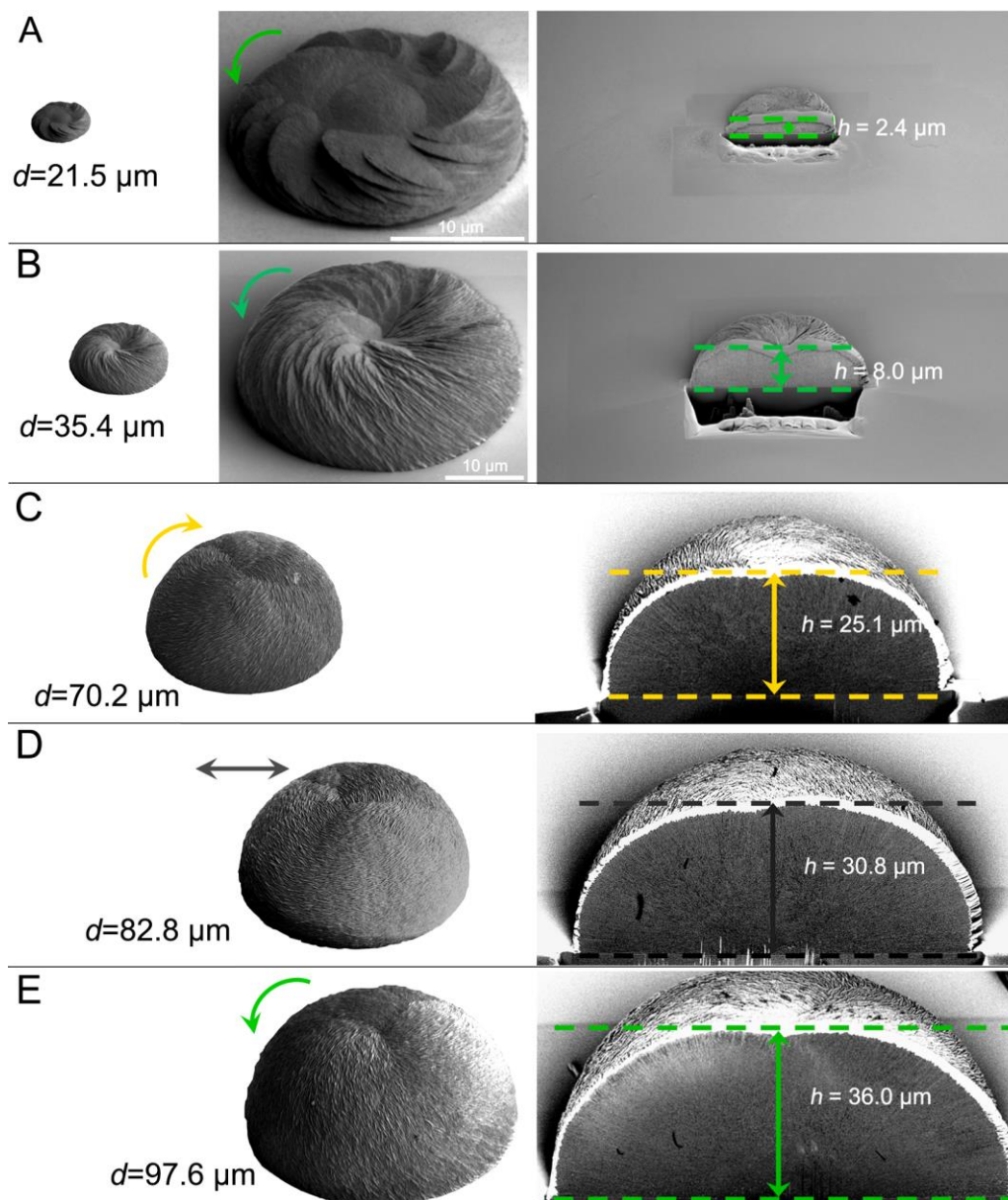


Fig. S4. Growth evolution of hierarchically organized vaterite helicoids with respect to size and height. SEM images of vaterite helicoids in the stage-one, inclined-platelet layer growth mode having initially a right-handed (counterclockwise, green arrows, **A** and **B**) orientation resulting from the nanointraplatelet tilting effect (19), to the second vertical platelet layer-by-layer rotation stage with “left-handed” (clockwise, yellow arrows, **C**) to the transitional achiral horizontal-surrounding vertical platelet orientation step (light gray double-headed arrow, **D**) and back finally to the “right-handed” direction (counterclockwise, green arrows, **E**), occurring through chiral switching induced

by the microinterplatelet effect in the presence of L-Asp enantiomer, as shown before and after FIB cutting which allows size and height (h) changes to be observed.

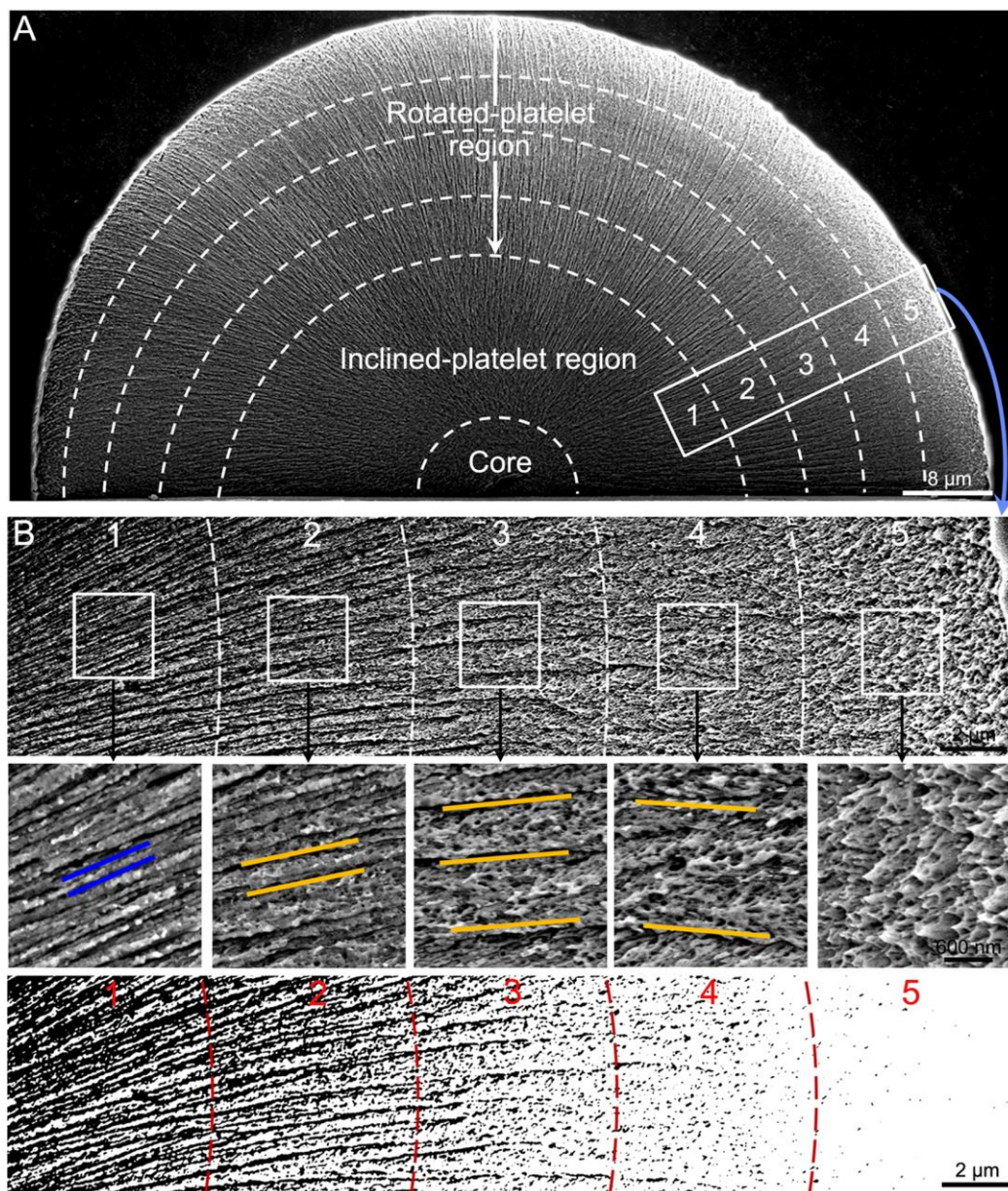


Fig. S5. Multilayering within chiral vaterite helicoids. (A) SEM image of a cross-section of a large achiral transitional helicoid (as shown in Fig. 5D in main text) with horizontal-surrounding vertical platelet orientation grown in the presence of L-Asp. The helicoid is composed of an initial

core disc/dome, an inclined-platelet region, and a rotated-platelet region with multiple vertical platelet layer-by-layer assembly structure. **(B)**, High magnification SEM images (including backscattered electron imaging, bottom row) of five adjacent platelet layers in the uppermost section of the inclined-platelet region and the whole rotated-platelet region of panel A. This shows the transition from sharp, on-edge views of platelets (panels B1) towards more diffuse, blurred density as the platelets rotate to the *en face* view (panels B5) in the outermost layer 5. Colored parallel lines illustrate increasing distances between platelet edges as they rotate towards the *en face* view.

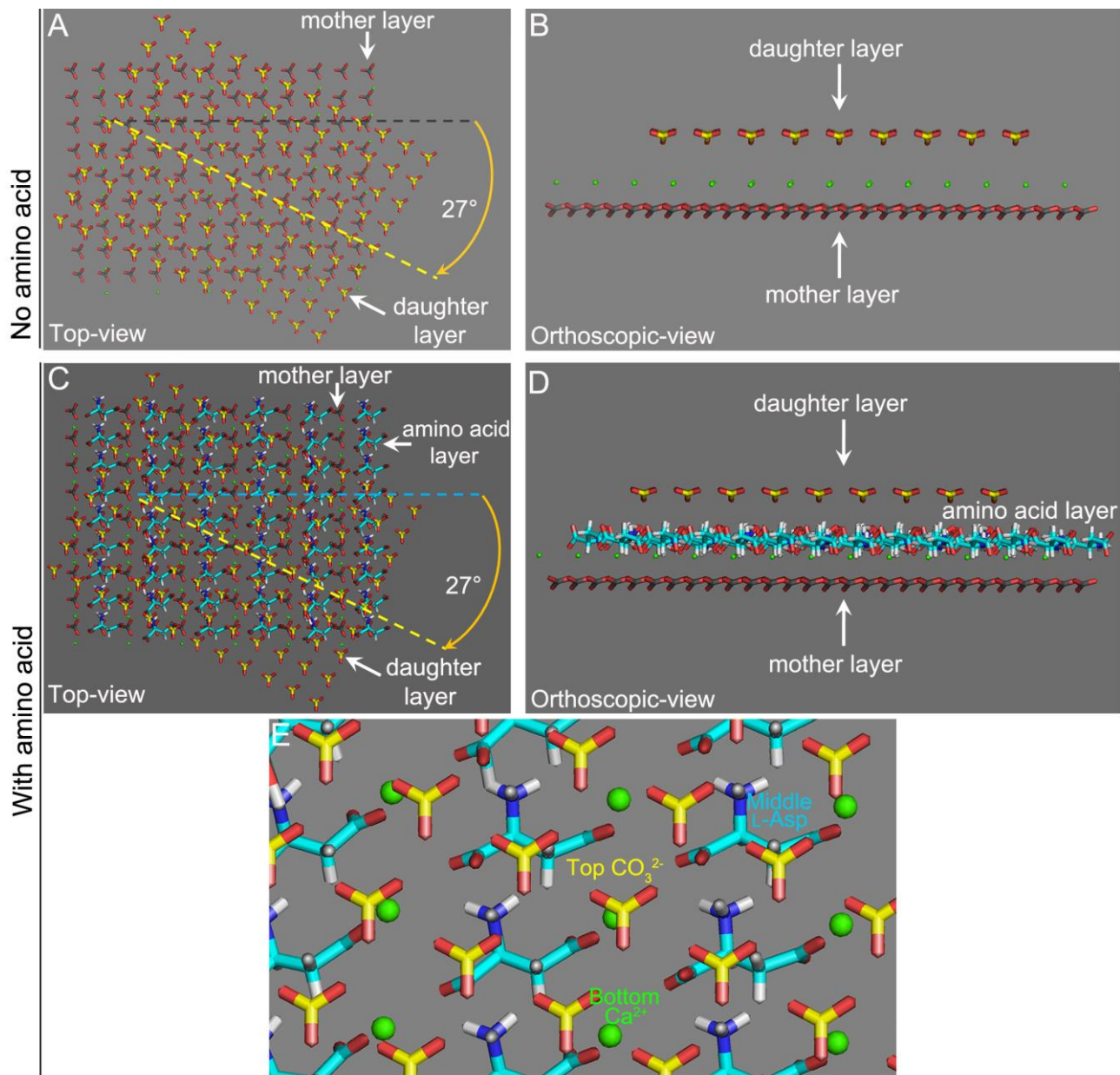


Fig. S6. Instability of adjacent rotated vertical vaterite platelets caused by the addition of chiral amino acid enantiomer. (A, B) Top-view and orthoscopic side-view schematics of a potential model at the (100) plane of the “daughter” vertical platelet layer (yellow) relative to the “mother” vertical platelet layer (gray) as identified by RosettaSurface simulation in the absence of amino acid, showing a clockwise rotation of $\sim 27^\circ$. At this rotation, the positively charged linear arrangement of calcium atoms (green) in the lattice of the “mother” vertical platelet layer top

surface locally aligns parallel to a linear arrangement of negatively charged carbonate groups on the "daughter" vaterite bottom surface, which suggests a local energy minimum at 27° . **(C, D)** Top-view and orthoscopic side-view of a potential unstable model of the "daughter" vertical platelet layer relative to the underlying L-Asp amino acid layer (light blue) organization as templated by the "mother" layer as identified by RosettaSurface computational simulation; this shows the clockwise rotation of 27° relative to the mother vaterite/L-Asp layer having a local linear parallel alignment between the negatively charged L-Asp arrangement and the negatively charged linear carbonate arrangement on the "daughter" vaterite bottom surface, whose repulsion leads to instability in the system. Thus, in order to decrease this repulsion that occurs in the presence of the acidic L-Asp layer, the model suggests that the 22.5° rotation that we observed experimentally (Fig. 6B in main text) would be energetically favorable compared to this 27° rotation. Vaterite crystal atoms: Ca, green; C, grey in "mother" layer and yellow in "daughter" layer; O, red. **(E)** High-resolution simplified image showing the configuration at the 27° rotation between the bottom "mother" vaterite layer with exposed surface calcium (green), the intervening middle L-Asp layer (blue), and the top "daughter" vaterite layer with exposed surface carbonates (yellow).

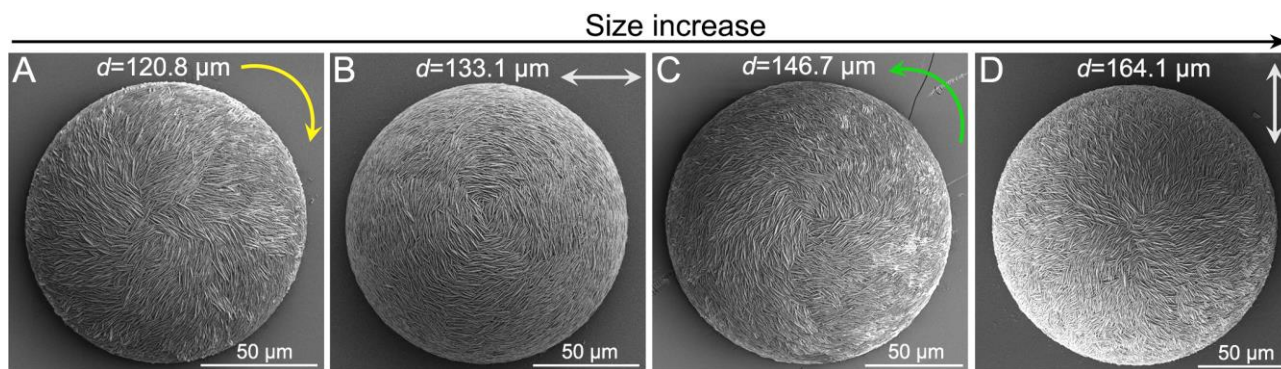


Fig. S7. Chiral switching by platelet layer-by-layer rotation correlates with size/growth of very large helicoids. SEM images of very large vaterite helicoids grown at long times (up to 3 months) formed by layer-by-layer rotation in the second growth cycle with typical successional clockwise (yellow arrow, **A**), horizontal-surrounding achiral (light gray double-headed arrow, **B**), counterclockwise (green arrow, **C**), and straight-radiating achiral (light gray double-headed arrow, **D**) orientations in the evolution process of helicoids grown in the presence of single L-Asp enantiomer, which are similar to those of vaterite helicoids formed in the first growth cycle as shown in main text Fig. 5, but with much larger sizes.

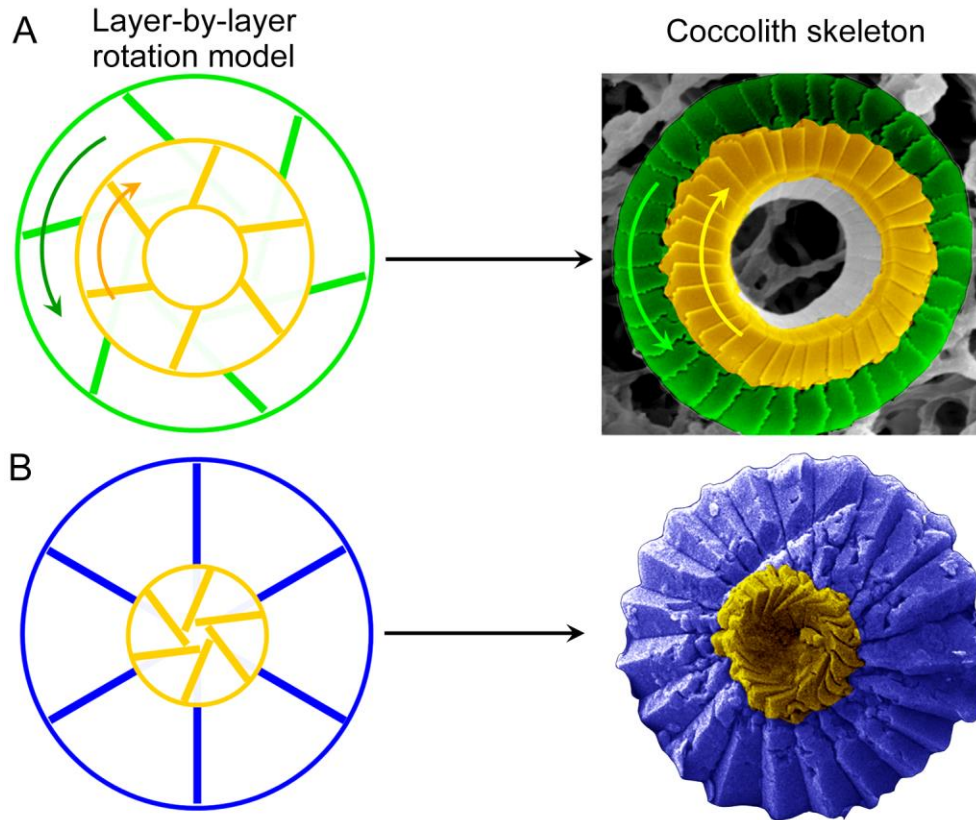


Fig. S8. Layer-by-layer growth models as a potential general strategy for switching chiral structures as observed in biology. (A) The model we propose could contribute to a reasonable mechanistic explanation for coccolith skeleton hierarchical structure where chiral switching is observed between apposed calcium carbonate layers (cycles), here as a bottom counterclockwise platelet layer (green) overlain by a top clockwise platelet layer (yellow) (*Umbilicosphaera foliosa* coccolith skeleton, ref. 9). (B) As another example, in *Discoaster salisburgensis* coccolith skeleton fossil (ref. 11) The model is consistent with the observed growth pattern showing a bottom achiral platelet layer (blue) and a top clockwise chiral platelet layer (yellow).

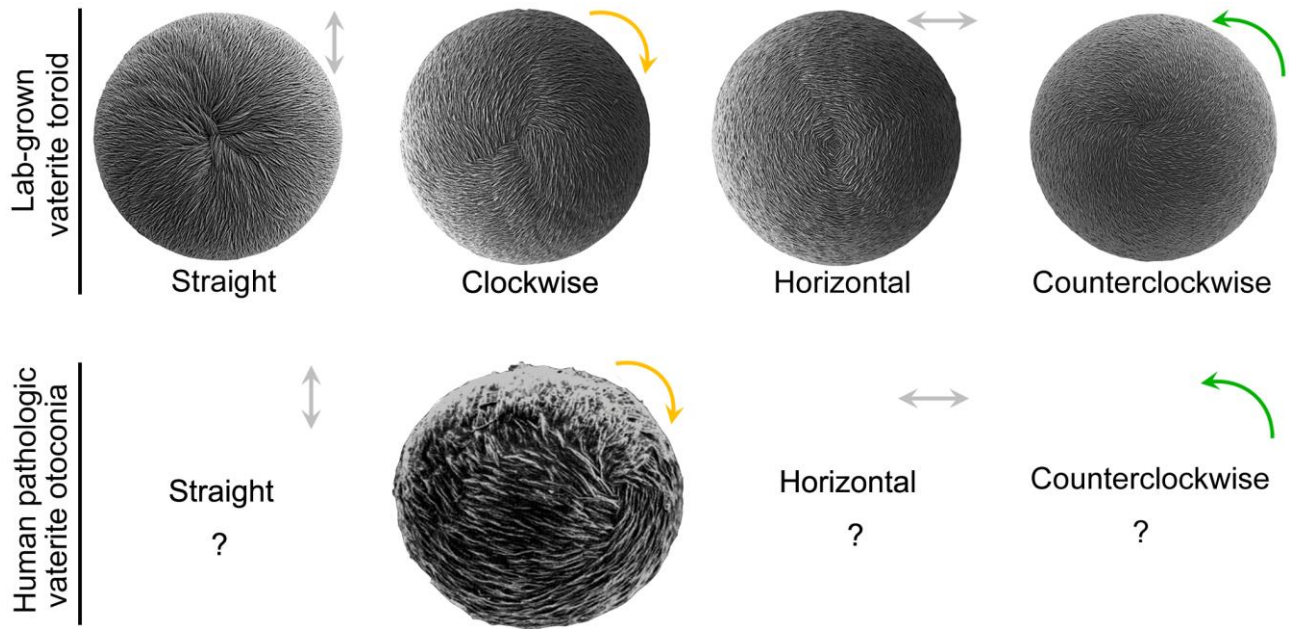


Fig. S9. Prediction of three as-yet unfound forms of human pathologic vaterite otoconia based on the vaterite helicoid chiral switching growth model. Based on the remarkable similarity between our synthetic lab-grown structures and an isolated observation of a human pathologic otoconia (Reprinted with permission from ref. 29), we propose that other otoconial vaterite forms could be found in humans having any of the additional three missing forms (?) that our model predicts: the first being a straight-radiating achiral form, the second being a counterclockwise form, and the third being the achiral horizontal-surrounding vertical platelet orientation form.

Supplementary Movie

Movie S1. Animation showing chiral switching in vaterite helicoidal suprastructures occurring by a vertical platelet layer-by-layer rotation mechanism in the presence of a single chiral enantiomer of acidic amino acid. Top-view 2D animation of the chiral switch occurring in vaterite helicoids where platelet layer-by-layer clockwise rotation by 22.5° occurs in the presence of L-enantiomer of amino acid (Asp) starting from the first achiral straight-radiating reference start-point at 0° (blue), to the clockwise organization ranging from 22.5° to 67.5° (yellow) from the start-point, then to second transitional achiral horizontal-surrounding platelet orientation at 90° (blue), then to the counterclockwise organization ranging from 112.5° to 157.5° (green), and finally then back to first straight-radiating point at 180° (blue) (left). The corresponding 2D successional rotated vertical platelet layers shown at the local level is shown on the right.